

This is the accepted manuscript version of the contribution published as:

Schirmer, M., Wink, K., Ohla, S., Belder, D., Schmid, A., Dusny, C. (2020):
Conversion efficiencies of a few living microbial cells detected at a high throughput by
droplet-based ESI-MS
Anal. Chem. **92** (15), 10700 – 10708

The publisher's version is available at:

<http://dx.doi.org/10.1021/acs.analchem.0c01839>

Conversion efficiencies of a few living microbial cells detected at high throughput by droplet-based ESI-MS

Martin Schirmer^{a#}, Konstantin Wink^{b#}, Stefan Ohla^b, Detlev Belder^b, Andreas Schmid^a, Christian Dusny^{a*}

^aHelmholtz-Centre for Environmental Research - UFZ Leipzig, Leipzig 04318, Germany. E

^bInstitute of Analytical Chemistry, Leipzig University, 04103 Leipzig, Germany

*Email: christian.dusny@ufz.de

Keywords: single-cell analysis, droplet microfluidics, chip-mass spectrometry, whole-cell biocatalysis

ABSTRACT: Label-free and sensitive detection of synthesis products from single microbial cells remains the bottleneck for determining the specific turnover numbers of individual whole-cell biocatalysts. We demonstrate the detection of lysine synthesized by only a few living cells in microfluidic droplets via mass spectrometry. Biocatalyst turnover numbers were analyzed using rationally designed reaction environments compatible with mass spectrometry, decoupled from cell growth, with high specific turnover rates (~ 1 fmol cell⁻¹ h⁻¹), high conversion yields (25%), and long-term catalyst stability (>14h). The heterogeneity of cellular reactivity of only 15 ± 5 single biocatalysts per droplet could be demonstrated for the first time by parallelizing droplet incubation. These results enable resolving biocatalysis beyond the averages of populations. This is a key step towards quantifying specific reactivities of single cells as minimal functional catalytic units.

■ INTRODUCTION

Microbial cells are used as biocatalysts in various fields of industry and academia as they enable complex multi-step chemistry at mild reaction conditions.¹⁻³ Their application as living and thus self-regenerating catalysts is often combined with high stereo-, chemo- and regioselectivity.^{4,5} In organic chemistry, whole-cell biocatalysts enable the design of elegant multistep one-pot reactions for the synthesis of fine chemicals or synthons.⁶⁻⁸ Optimizing biocatalytic syntheses towards certain objectives requires a fundamental understanding of the underlying cell-specific mechanisms. Currently, biocatalyst analysis is advancing from population-based values towards single cells for understanding catalytic processes in detail, including cellular heterogeneity in terms of reactivity and turnover numbers.⁹⁻¹⁶ The determination of cell-specific reaction rates and yields is however highly challenging, due to the low amounts of catalytic products.

Lab-on-a-chip technologies unite cultivation, incubation, sampling, and ultra-sensitive analysis of minute sample volumes and analyte amounts on one single chip-sized device.¹⁷⁻²¹ Integrated microfluidics thus provide a promising instrument for analyzing the efficiencies of whole-cell biocatalysts at its minimal level. Next to sensitivity, a high analytical throughput is necessary for quantifying the spectrum of cell-specific reactivity in a statistically meaningful way.²²

Droplet-based microfluidic systems allow the miniaturization of catalyst screening and utilize water-in-oil enclosed droplets as sub-nL reaction vessels. Biocatalytic products accumulate in the droplets serving as highly parallelized miniaturized batch reactors.²³⁻²⁴ Various detection methods can be applied for analyzing distinct analytes in droplets, but are most often restricted to optical readouts such as fluorescence spectroscopy.²⁵⁻²⁹ Label-free analytical methods are required for overcoming the restriction of investigating exclusively fluorescent products. The most powerful method comprises the highly selective and sensitive, label-free detection of biocatalytic products via mass spectrometry (MS), which could be coupled already with droplet microfluidics.³⁰⁻³⁵ Matrix effects are however critical for the sensitivity of MS analyses. The composition of the reaction medium has to satisfy the requirements of both the biocatalyst and the MS for analyzing products at the single-cell level. Ideally, the biocatalytic reaction has to be carried out in an ESI-MS-compatible medium. This is in sharp contrast to conventionally used salt-rich microbial cultivation media, which strongly suppress analyte ionization.³⁶⁻³⁹

We present a novel methodological concept for next-generation label-free analysis of whole-cell biocatalysts on a cellular level. Droplet/chip-coupled mass spectrometry technology was brought to application as a powerful tool for analyzing a multi-step reaction from

glucose to lysine catalyzed by only a few living biocatalysts in sub-nL droplets. *Corynebacterium glutamicum*, a biocatalytic workhorse for the production of amino acids, was investigated as a model strain. The 28-step conversion of D-glucose to L-lysine by *C. glutamicum*⁴⁰ served as a target for tracing biocatalysis with only a few cells for the first time, enabled by an integrated lab-on-chip/MS approach. We chose this specific biocatalyst as it is one of the most important whole-cell biocatalysts for industrial biotechnology. The strain DM1919 was optimized for L-lysine production via extensive metabolic engineering and is one of the most reactive known strains and offers the required high cell-specific reaction rates to demonstrate the feasibility of our approach.⁴⁰ Whole-cell biocatalysts were incubated in a non-conventional reaction medium with subsequent microfluidic on-chip incubation by dead-volume free ESI-MS detection of reaction substrate and product. The turnover number of whole-cell biocatalysts (its biochemical activity) and its reactivity (summarizing mass transfer, stability, and other reaction parameters) were screened in different volatile reaction media and were highest in ammonium bicarbonate.

■ Experimental Section

Cell cultivation of *Corynebacterium glutamicum*

Precultures of recombinant *Corynebacterium glutamicum* DM1919 pSenLys cells were routinely prepared in BHI complex medium (brain-heart infusion, 37.5 g/L).^{40,41} After overnight incubation at 30°C, the precultures were used to inoculate CGXII mineral medium containing 20 g/L (NH₄)₂SO₄, 1 g/L K₂HPO₄, 1 g/L KH₂PO₄, 5 g/L urea, 13.25 g/L CaCl₂ · 2 H₂O, 250 mg/L MgSO₄ · 7 H₂O, 30 mg/L protocatechuic acid, 0.2 mg/L biotin, 10 mg/L FeSO₄ · 7 H₂O, 10 mg/L MnSO₄ · H₂O, 0.02 mg/L NiCl₂ · 6 H₂O, 0.313 mg/L CuSO₄ · 5 H₂O, 1 mg/L ZnSO₄ · 7 H₂O and 10 g/L D-glucose.⁴² Additional 50 mg/L kanamycin sulfate (Km) was added to prevent loss of the YFP-gene carrying plasmid. The mineral medium precultures were used to inoculate CGXII medium for subsequent main cultures. The biocatalyst cells were incubated in baffled Erlenmeyer flasks (100 mL) in horizontal shakers at 30 °C and 180 rpm (INFORS HT, Bottmingen, Switzerland, Ø 50mm). After cultivation for 8 h, the main culture was centrifuged twice (1 min, rt, 13750 g), the supernatant discarded and washed twice with the respective ammonium-based reaction medium. For activity assays and droplet incubation, the cell pellet was resuspended in the corresponding reaction medium (AC, AF or AA) and diluted to the desired biocatalyst concentration.

Activity assays in ammonium-based reaction media

20 mL of biocatalyst suspension in the corresponding reaction medium (OD₆₀₀ ~ 1 (Biochrom Ltd., Cambridge, UK)) were transferred to baffled Erlenmeyer flasks (100 mL). D-glucose (0.5 or, respectively 2 g/L) was added to start the reaction. The biocatalyst culture was incubated

in horizontal shakers at 30 °C and 180 rpm. 1 mL samples were taken 10 min after adding glucose, followed by hourly sampling intervals. After measuring OD₆₀₀ with a photometer and cell concentrations with a Coulter Counter device (Beckmann Coulter Counter), the remaining biocatalyst suspension was centrifuged (10 min, 17000 g, 4 °C). The supernatant was taken and analyzed via HPLC (Thermo Scientific Dionex Ultimate 3000 HPLC). Analyte separation was performed using a Sielc Primesep 100 (Sielc Technologies, 4,6 to 250 mm, 100 Å pores, 5 µm pore diameter) and detection was carried out with a charged aerosol detector (CAD) (Thermo Fischer Corona). Acetonitrile, supplemented with 0.1% (v/v) formic acid and 0.4% (v/v) trifluoroacetic acid was used as the mobile phase. The column temperature was set to 32°C and eluents were pumped with a flow rate of 1.5 µL/min. Details on fluorescence time-lapse microscopy and chip fabrication can be found in the supporting information (SI).

Droplet-based on-chip incubation and chip/ESI-MS

The chip/MS operation was done similar to earlier work.⁴³ A Shimadzu LCMS-2010 mass spectrometer was used. After the removal of the commercial ionization source, the microfluidic chip was positioned in front of the mass spectrometer inlet using a home-built interface frame with an XYZ-positioning stage (OWIS, Germany). The temperature of the heating block was set to 200 °C, while the temperature of the curved desolvation line was set to 250 °C. The potential at the curved desolvation line was set to 0 V. The mass spectrometer was operated in positive scan mode (50-250 m/z) with a data acquisition frequency of 25 Hz. Mass spectra were recorded in scan mode using the vendor's software. Chip emitter and counter plate potentials were applied with a four-channel high-voltage power supply HCV 40 M-10000 (FuG Elektronik GmbH, Germany). For the droplet-based incubation, 2 g/L of D-glucose was added to cultivated cells which were suspended in 10 mM AC. Thirty minutes after D-glucose addition, the suspended cells were encapsulated into droplets with an aqueous sample flow rate of 1.0 µL/min and an oil flow rate of 2.0 µL/min using a T-junction generating droplet volumes of ~ 1 nL. The used oil was FC-40 with 2% "pico surf 1" (Sphere Fluidics, UK). Fluids were pumped to the chip via pressure pumps (MFCS-EZ and flow units by Fluigent, Germany). After filling of the on-chip incubation chamber with encapsulated cells, fluid flows were stopped for subsequent incubation over 8 hours. After incubation, oil flow was set to 0.5 µL/min while the flow rate of the spacer oil was set to 1 µL/min. The emitter potential for electrospray was set to 2.7 kV. Blank samples were measured by immediate droplet/ESI-MS detection after cell encapsulation. Droplet data analysis was done with Data Analysis (Bruker Daltonik GmbH, Germany). Data plotting was done with Origin Pro 2017 (Origin Lab, USA).

RESULTS

A schematic overview of the presented work is shown in Figure 1A-B. The bacterium *Corynebacterium glutamicum* was used as a model system which catalyzes the enantioselective 28-step synthesis of L-lysine from D-glucose (“lysine” and “glucose” in the further text). The methodological concept for the label-free detection of catalytic products from a few living microbial whole-cell biocatalysts comprises three pillars (Figure 1C-E).

Firstly, volatile, aqueous reaction systems need to stabilize the reactivity of biocatalysts over several hours (Figure 1C). Reaction systems that enable both cellular biocatalytic activity and analyte ionization were designed and validated for the detection of low-abundant lysine via ESI-MS. The second pillar comprises the design and application of a droplet-based microfluidic device for parallelized cell incubation at the sub-nL scale (Figure 1D). Thirdly, a dead-volume free chip/MS interface transfers droplets seamlessly to the MS detection (Figure 1E).

The functionality of the newly developed reaction media was validated with different types of common microbial biocatalysts.

Ammonium-based matrices enable whole-cell catalysis in MS-compatible environments

Cellular biocatalysts are usually cultivated and characterized in complex salt-rich, non-volatile aqueous buffer systems in a pH-range of seven to eight for cell viability and high metabolic activity. However, in ESI-MS analyses, mineral media matrices cause analyte ion suppression, which dramatically hampers the sensitivity of MS analyses. Specifically, minimal media like CGXII³⁶

for *C. glutamicum* prevent lysine ionization and hence detection (Figure S1 in the Supporting Information shows the MS response comparison between CGXII medium and a volatile medium). Alternative volatile reaction media may help to overcome the issue of matrix-induced ion suppression. A reaction system had to be designed that does not involve matrix effects during ESI and simultaneously allows high catalytic performance of the cells. Based on these requirements, aqueous ammonium acetate (AA), ammonium formate (AF) and ammonium bicarbonate (AC) solutions were chosen as potential reaction systems as the salts are volatile. For microbial cells, ammonium serves as a nitrogen source for lysine synthesis. Biocatalyst reactivity and stability were investigated in the chosen aqueous reaction systems in flask experiments. The salt concentration was adjusted to 10 mM for achieving physiological reaction conditions and to prevent osmotic imbalances. Averaged cell-specific catalytic activities were measured by quantifying the glucose to lysine conversion via HPLC. Glucose was added to the cell suspension with a starting concentration of 0.5 g/L, while the catalyst concentration was set to $2.1 \cdot 10^{11}$ cells/L. Whole-cell biocatalysts showed constant glucose uptake and lysine production over a period of 3 h in AC solution, but no detectable catalytic activity in AA and AF (Figure 2A). After complete consumption of glucose in AC, lysine production stopped, lysine was not further metabolized despite the lack of a carbon and energy source for the cells. These results demonstrated that the biocatalytic synthesis of lysine by living cells is possible in simple, MS-compatible reaction environments.

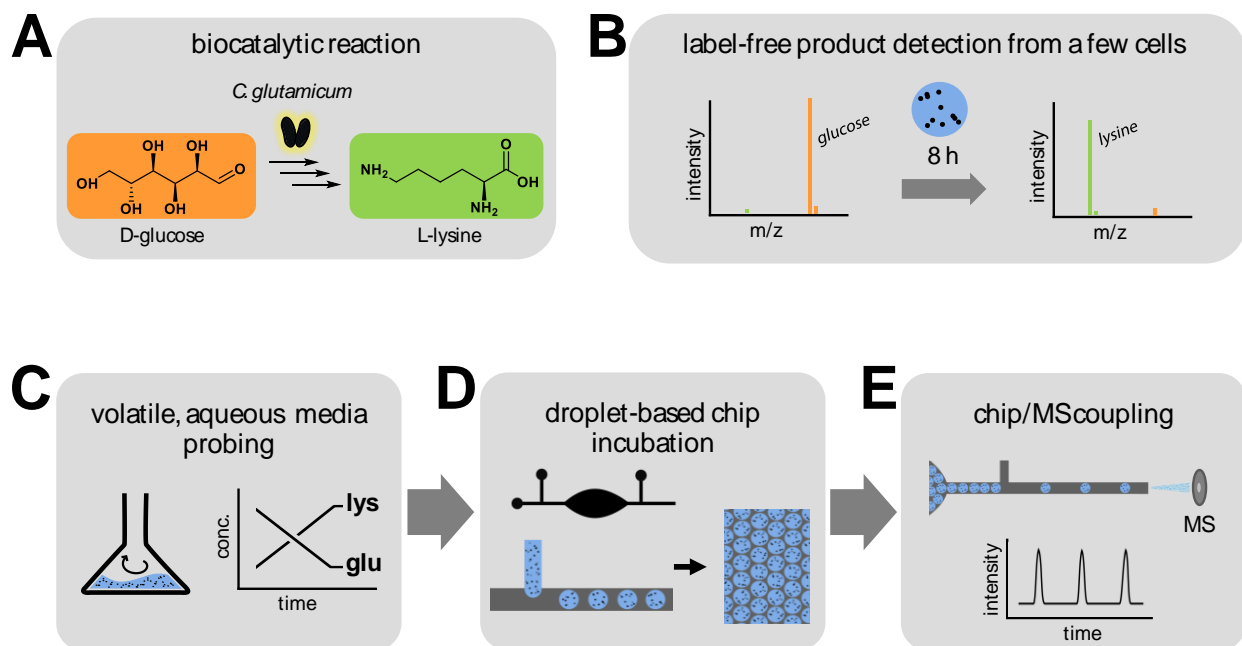


Figure 1. Schematic overview of (A) the biocatalytic reaction of glucose to lysine catalyzed by *Corynebacterium glutamicum* and the subsequent (B) label-free detection of lysine in single droplets by ESI-MS after a reaction time of 8 h. (C) Workflow including probing of volatile media for biocatalyst performance. With the successfully probed ammonium bicarbonate reaction medium, (D) a droplet-based incubation was conducted in chambers in a microfluidic chip. (E) After incubation, droplets were spaced and injected one by one into a mass spectrometer for label-free analysis via ESI-MS.

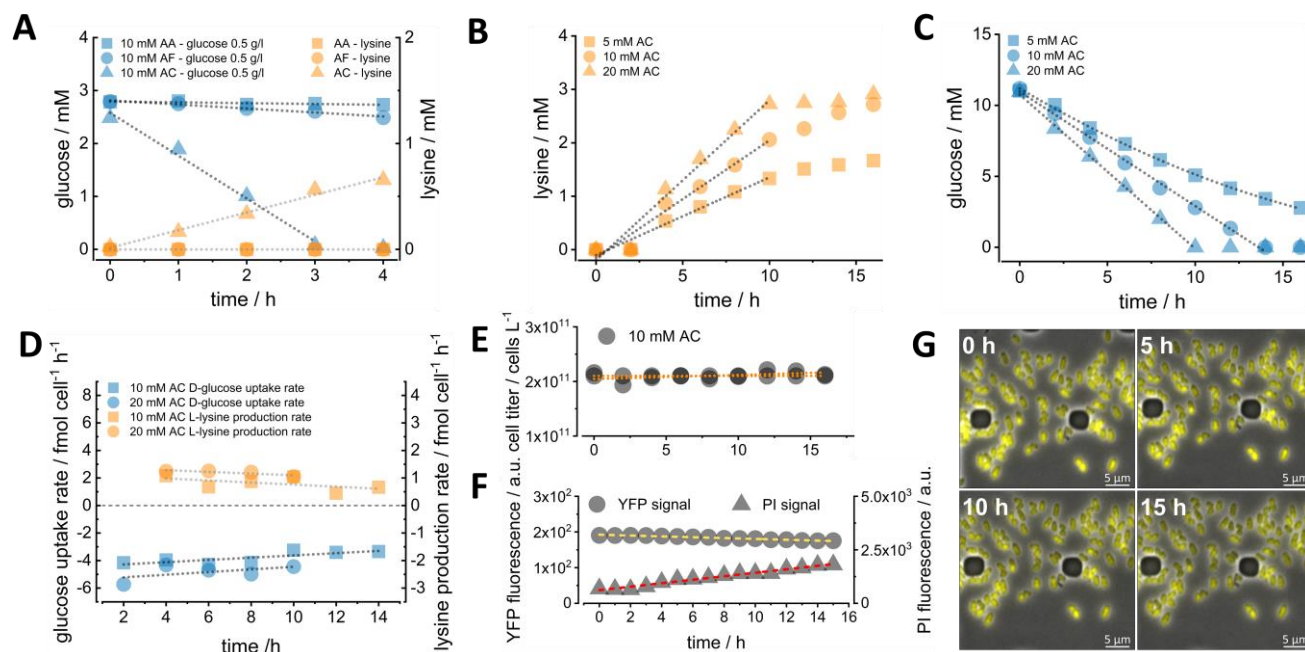


Figure 2. (A) Glucose uptake and lysine production of *C. glutamicum* in ammonium acetate (AA), formate (AF) and bicarbonate (AC) (10 mM, respectively) via bioassays in shaking flask experiments and subsequent HPLC with a cell titer of $2.1 \cdot 10^{11}$ cells/L. Only AC showed significant glucose consumption and lysine production. (B) Lysine production and (C) glucose uptake in 5, 10 and 20 mM AC over 15 h. (D) Glucose uptake and lysine production rate over 14 h in 10 and 20 mM AC. (E) Cell titer in 10 mM AC over the course of 16 h. (F) Mean intensity of YFP and DNA-intercalated propidium iodide fluorescence in *C. glutamicum* over 16 h via fluorescence time-lapse microscopy. (G) Photographs of biocatalysts at 0, 5, 10 and 15 h overlaid with the corresponding YFP fluorescence signal of each biocatalyst.

Turnover numbers were determined in activity assays in reaction media with different AC concentrations for evaluating the effect of the AC concentration on the whole-cell catalysts. AC concentrations were varied between 5 mM and 20 mM with 2 g/L glucose as reaction substrate. The catalytic activity of the cells scaled with increasing AC concentration. The biocatalyst activity in terms of lysine production (Figure 2B) and glucose uptake (Figure 2C) was unaffected by the reaction medium environment and concentration. Adding a minuscule amount (1/1000 vol-%) of growth medium to the AC reaction medium resulted in no measurable differences in terms of biocatalyst activity compared to sole AC solution (Figure S4 in Supporting Information). Average single-cell specific glucose uptake and lysine production rates were estimated from the flask experiments. A glucose uptake rate of ~ 4 fmol-cell⁻¹h⁻¹ and a lysine production rate of ~ 1 fmol-cell⁻¹h⁻¹ were determined with a specific lysine yield on glucose of 25% mol/mol (Figure 2D). Based on these estimated rates, one single cell in a 1 nL droplet volume yields a lysine concentration increase of ~ 1 μ M after 1 h of incubation.

Product formation rates of two other biocatalytic strains were examined as well to demonstrate the broad applicability of volatile reaction media for whole-cell biocatalysis. Using AC, catalytic activity could be detected for the biotransformation of L-proline to trans-4-hydroxyproline with a modified *E. coli* strain (Δ putA(DE3) (pET_p4h1of)⁴⁴). The protein-producing yeast *H. polymorpha* (RB11 MOX-GFP)⁴⁵ was able to

synthesize green fluorescent protein from glucose in AF (see Supporting Information for further details, Figure S2, and S3, respectively). These results indicate that the developed ammonium-based media are well suited as reaction environments for a broad variety of microbial biocatalysts and types of catalytic conversions under MS-compatible conditions.

The catalytic capacity of the cells could be analyzed uncoupled from biological factors such as growth as the whole-cell catalyst did not replicate during the reaction. Neither cell growth nor cell division was observed for *C. glutamicum* due to the nutrient-limited environment in AC reaction medium (Figure 2E). The cell concentration remained constant. The fate of individual whole-cell biocatalysts in terms of cell viability in the AC environment was followed by fluorescence time-lapse microscopy (Figure 2F-G). During these experiments, constant environmental conditions were applied in a flow-based microfluidic cultivation system. Discrimination of live and dead cells was performed using propidium iodide (PI) staining, which was added to the AC medium. The PI signal hardly increased during 15 h of cell incubation in AC assay (Figure 2F). PI staining is resulting in bright red fluorescence from DNA intercalation. PI can only pass permeabilized cell membranes and thus indicates non-intact cells. This result thus demonstrates the viability of *C. glutamicum* cells even after extended incubation periods > 15 h in AC buffer.

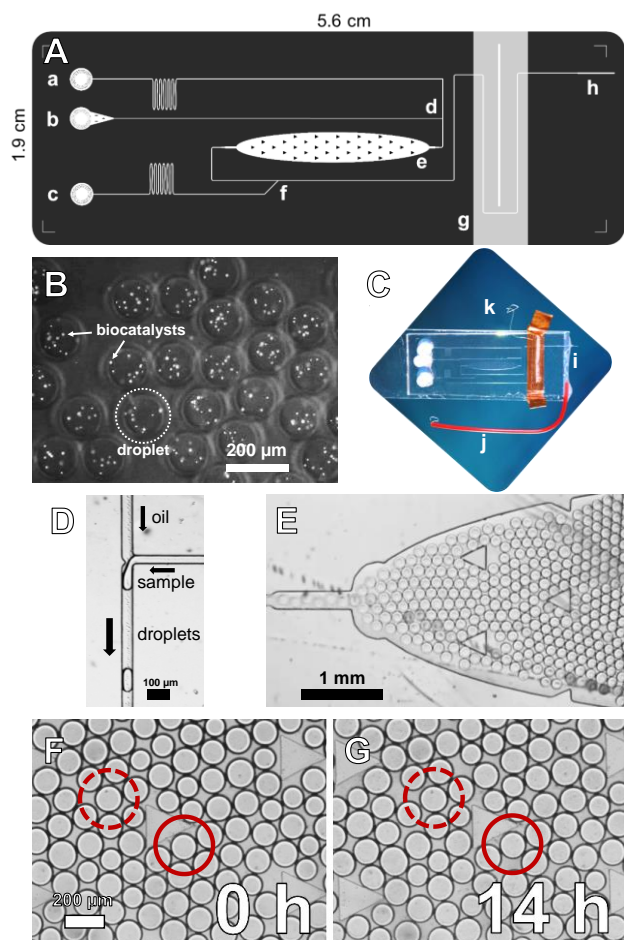


Figure 3. (A) Used microfluidic chip design with inlets for fluorinated oil (a, c) and biocatalyst suspension (b), T-junction for droplet generation (d), droplet incubation chamber (e), droplet spacing junction (f), electric shielding area (g) and channel-to-emitter transition (h). (B) Photograph of encapsulated, YFP expressing *C. glutamicum* cells (bright spots) in droplet volumes of ~1 nL. (C) Photograph of the microfluidic chip with an integrated steel emitter (i), electric contact of the emitter (j) and an electric shielding area (k). (D) Photograph of the droplet generating T-junction. (E) Photograph of the droplet incubation chamber. (F) Photograph of droplets at 0 h and (G) at 14 h inside the chamber.

Integrated microfluidics enable spatio-temporal droplet control

The reactivities of only a few living cells were analyzed using droplet microfluidics. Droplets were used to encapsulate *C. glutamicum* biocatalysts in 10 mM AC. Whole-cell biocatalysts were compartmentalized into aqueous droplets surrounded by fluorinated oil and an on-chip droplet incubation over several hours with a dead-volume free coupling of chip/ESI-MS for lossless droplet transfer. The developed PDMS/glass chip integrates these properties and is described in Figure 3. The channel design of the chip is shown in Figure 3A, enabling cell encapsulation and storage of biocatalyst-loaded droplets (Figure 3B). A photograph of the assembled chip with an ESI emitter is shown in Figure 3C. For the encapsulation of cells, a conventional T-junction (Figure 3A/d and Figure 3D) was used to generate

droplets with adjustable volumes (~ 1 nL). In order to accumulate synthesized lysine inside the droplets, an incubation over several hours was employed in an incubation chamber (Figure 3A/e, Figure 3E and Supporting Information videos V1 and V2). In abiotic experiments, droplet crosstalk in terms of lysine was excluded (data not shown). With this strategy, ~ 500 droplets could be simultaneously stored and were stable for at least 14 h (Figure 3F/G). Due to the constitutive YFP (yellow fluorescent protein) gene expression of the used biocatalytic strain, cells could be counted when the flow was stopped (Figure 3B). As expected, the heterogeneity of cell concentrations in individual droplets followed a Poisson distribution⁴⁶ (see Supporting Information Figure S5). After incubation, the stored droplets were spaced with a second oil channel for transferring single droplets into the MS. Due to the relatively low sampling rate of the used MS instrument (25 Hz), droplets were injected at a frequency of 1-2 Hz to achieve a discrete signal for each droplet.

Detecting product formation of only a few living cells encapsulated in individual droplets with chip-ESI-MS

Chip/MS coupling was utilized for lossless droplet transfer.⁴⁷ Single droplets were electrosprayed from an integrated steel emitter. This enabled a direct and dead-volume free transfer of sub-nL samples to the MS. To generate an electrospray, the chip emitter was aligned with an oppositely positioned counter plate electrode (Figure 4A). The counter plate axis was positioned perpendicular to the MS inlet to prevent contamination of the MS with oil.⁴³

The chip-MS interface was adjusted in relation to a suitable potential and geometry to stabilize the Taylor cone formation at the emitter tip. The corresponding sawtooth-like signal trace of the individual droplets is shown in Figure 4B and 4C. Droplets containing 100 μM lysine in 10 mM AC were generated on-chip and subsequently electrosprayed to prove the feasibility of this method. The spatial separation of the droplets was deduced from the resulting signal traces as the frequency of the ejected droplets matched the detected droplet frequency in the recorded ion trace. The intensity drop between neighboring peaks correlated with the ejection of the oil phase (Figure 4D). Each peak corresponds to a distinct electrosprayed droplet with a corresponding mass spectrum (Figure 4E; the m/z value of protonated lysine is marked as [lysine+H]⁺). Excessive oil was removed with an additional PTFE tubing drain in close proximity to the emitter orifice. The electric field caused by the emitter/MS configuration was shielded from the incubation chamber by wrapping a grounded copper stripe around the chip for preventing electro-induced droplet coalescence.

The combination of the developed methodological pillars enabled the analysis of *in situ* lysine production by a few *C. glutamicum* cells. The cell titer of the seeding suspension was adjusted to encapsulate ~15

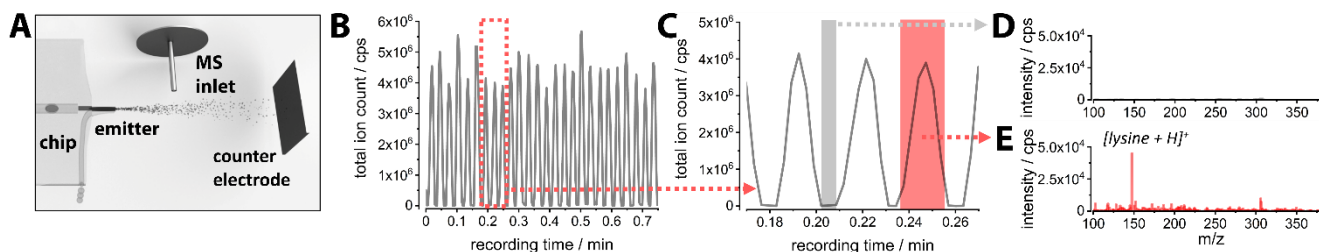


Figure 4. (A) Schematic chip/MS coupling consisting of an integrated chip emitter protruding from the chip spraying against a counter electrode while ions were collected by an MS inlet in vertical arrangement. (B) Corresponding total ion count (TIC) detected by the MS showing a typical sawtooth trace where a valley corresponded to the arrival of oil at the emitter while a peak corresponded to an electrospray of a droplet generating a mass spectrum for each droplet. (C) Magnification of (B). (D) Mass spectrum of the fluorinated oil. (E) Mass spectrum of a droplet containing 100 μM lysine in 10 mM AC.

biocatalysts/droplet on average. 400 μM glucose served as reaction substrate. Droplet incubation was conducted over eight hours at room temperature. After incubation, droplets were injected one by one into the MS and discrete mass spectra of single droplets could be obtained. A normalization of the recorded signals was performed by tracing the lysine/glucose signal intensity fraction of single droplets to compensate for signal intensity fluctuations. Figure 5A shows the lysine/glucose ratio at the start of reaction and after eight hours of incubation. In the exemplary mass spectrum at the start (Figure 5B), the corresponding glucose signal marks the base peak and decreases significantly after eight hours of incubation, indicating that the biocatalysts consumed the glucose inside the droplet. An increase of the corresponding lysine signal was detected after eight hours, indicating lysine synthesis. The comparison with standard spectra excluded that further products or cell metabolites were formed in larger quantities (S7).

In order to probe the heterogeneity among the incubated cells with respect to reactivity, a semi-quantitative analysis of substrate to product signal responses was performed. Initially, artificial matrices spiked with different ratios (1:1, 2:1, 1:2) of lysine and glucose in 10 mM AC were analyzed via chip-coupled droplet MS. The standards show a relatively narrow distribution of intensity ratios in comparison to the cell-based reaction monitoring (Figure 5A). Minor lysine signals were detected at $t = 0$ h of the reaction but showed a narrow distribution of intensity ratios. The recorded peaks were hence a result of lysine carryover from catalyst preparation. After 8 h of droplet-based catalyst incubation, the detected lysine/glucose distribution was much broader than for artificial standards. These results demonstrate the significance of biological heterogeneity as a determining factor for the reactivity of whole-cell biocatalysts.

DISCUSSION

Label-free analysis of reactivity of microbial whole-cell biocatalysts is now possible at the level of a few living single cells. This opens novel possibilities to study whole-cell biocatalysis at its minimal possible level. Latest findings suggest that catalytic heterogeneity among

isogenic cells might have a dramatic effect on the conversion efficiency of the population, but catalytic heterogeneity is a yet poorly understood aspect of whole-cell biocatalysis.⁴⁸ It is, therefore, particularly important to control and engineer heterogeneity to establish novel, more efficient biocatalytic processes.¹⁵ However, up to now, it is not possible to detect catalytic heterogeneity at the level of a few or even a cell. By extending the analytical window of cellular assays inside microfluidic droplets beyond spectroscopic readouts, a much wider range of target molecules can be subjected to scientific questions in the omics/ESI-MS field, such as the quantitative and qualitative elucidation of cellular metabolic fluxes, as no labelled flux sensors are necessary.^{49–51} Additionally, no further purification steps prior to ESI-MS are needed. The presented work demonstrates the parallelized analysis of biocatalyst performance and heterogeneity via label-free mass spectrometry at the lowest reported level. In contrast to other breakthroughs in microbial single-cell mass spectrometry^{9,13}, our approach grants access to statistically relevant data on catalytic heterogeneity among cells for the first time. Combining a universally applicable bio- and MS-compatible reaction medium with MS-coupled droplet microfluidics is the key to achieve reaction monitoring in sub-nL reaction volumes. The absence of other essential nutrients in the reaction systems suppressed biocatalyst proliferation. This enables studying the reactivity of whole-cell biocatalysts uncoupled from biological phenomena such as biomass growth. Bacterial whole-cell biocatalysts showed the highest activity in AC reaction media, while yeast was most active in AF. This observation can be attributed to cell-specific physiological responses to pH values below 7 or anions like formate and acetate.^{52–55} Yeast, on the other hand, was active in AF as it prefers low pH values and is able to metabolize formate as carbon and energy source.^{44,56} These results demonstrate that volatile buffer systems can be applied for catalysis with several different types of catalysts. Parameters such as ionic strength, volatility and pH have to be taken into account when customizing buffers and adjusted to specific cells requirements. However, the presented buffers can be used in a modular fashion to enable catalysis under MS-compatible reaction conditions when considering these aspects.

The turnover number (activity) of *C. glutamicum* in AC was in the same order of magnitude as compared to conventional cultivation media (CGXII).⁴⁰ Cell stability was sufficient to achieve a full consumption of glucose within 14 h of incubation. The molar yield of lysine on glucose was 25%, while it can reach up to 40% in growth medium. This loss in yield can be explained by an increased energy-intensive cell metabolism and maintenance in the reaction medium.⁵⁷

The rates calculated from the results of the Resting Cell Assay (RCA) allowed us to rationally design droplet experiments in terms of cell loading and incubation times. The amount of ammonium ions needed for the production of ~ 1,5 mM lysine is ~ 3 mM for the reaction with 2 g/L glucose. This corresponds to 60%, 30% and 15% of the ammonium ions that were present in the 5, 10 and 20 mM reaction media, respectively. Further ammonium might have been consumed as a nitrogen source for the physiological maintenance of the cell. This resulted in successively decreasing glucose uptake and lysine production rates in the flask experiments with 5 mM and 10 mM. However, the molar amount of AC per cell was more than 10 times higher in the droplets than in the shake flasks. Limitation effects in droplets due to AC depletion can thus be excluded. This now allows a reduction of AC concentration in future experiments for minimizing ion suppression and for further enhancing the sensitivity of the method for reaching the single-cell level.

Catalyst stability in AC was confirmed by time-lapse microscopy. The observed decrease of the fluorescence signal correlated well with the decrease in the specific rates of glucose uptake and lysine production and stemmed from bleaching effects due to fluorescence excitation. Cell integrity could be maintained for all tested types of biocatalysts. Cell encapsulation followed a Poisson distribution. This allowed the loading of the droplets with defined numbers of individual cells. Droplet incubation was sufficiently stable for incubation times of at least eight hours. This means that a large span of cell-based catalytic processes with different incubation times can be covered with the analytical concept. Droplet coalescence could be prevented by the addition of a non-ionic emulsion-stabilizing surfactant.³⁴ Shrinkage of the droplets caused by minor evaporation through PDMS was less than 5% of the droplet volume during incubations over ten hours. This demonstrated the feasibility of droplet storage (Supporting Information, Figure S6). In addition, oxygen availability can be excluded as a rate-limiting process due to the high solubility of oxygen in fluorinated oils.⁵⁸

Droplet-chip/MS experiments were designed based on the averaged activities (~1 fmol cell⁻¹ h⁻¹) that could be calculated with biocatalyst populations in shake flask reactions. 15±5 catalysts/droplet were encapsulated inside the investigated droplet bioreactors for incubation over several hours to reach detectable amounts of lysine inside the droplets. A theoretically calculated amount of glucose was added that should have been consumed by 10 cells within 10 hours to ensure full conversion of glucose

to lysine. However, glucose was still present in small amounts inside droplets after 8 h of incubation. This might be caused by droplet incubation in front of the MS instrument at 21-22°C, which is 8-9 °C lower compared to shake flask experiments. The microfluidic chip was positioned in front of the MS instrument during the incubation because chip movement could lead to droplet ejection out of the chip. Therefore, a decrease in catalytic lysine production of up to 50 % in the droplet/ESI-MS experiments was expected due to a lower on-chip reaction temperature. To achieve higher sensitivity, interfering matrix effects (such as the peaks next to glucose and lysine in Figure 5B) can be minimized by employing ESI emitters with a smaller diameter than 50/100 µm (i.d./o.d.).⁵⁹ However this increases the risk of blocking the emitter and might lead to a higher pressure build-up which disrupts the droplet manipulation in the

chip. The conversion ratio of corresponding product-to-substrate (lysine/glucose) signals in individual droplets was used for evaluating the reactivity of the investigated *C. glutamicum* biocatalysts.^{60,61} Fractional analyses were utilized to compensate electrospray instabilities which occur during MS analyses of segmented flow samples^{34,47}. The results of the droplet-based cell experiments point towards significant heterogeneity of catalytic activity among cells, which could be detected at the few cell-level for the first time. Future works will focus on disclosing cell heterogeneity in terms of reactivity in detail by quantifying with isotopically labelled standards. This

further extending the cell incubation times might be final measures to reach the single-cell level with our platform. We are confident that the sum of these actions will enable label-free secretome analysis of single microbial whole-cell biocatalysts in the near future.

CONCLUSION

Catalytic processes in only a few living cells can now be analyzed and resolved with droplet-based mass spectrometry. The possibility of studying whole-cell biocatalysis at the single-cell level is now closer than ever

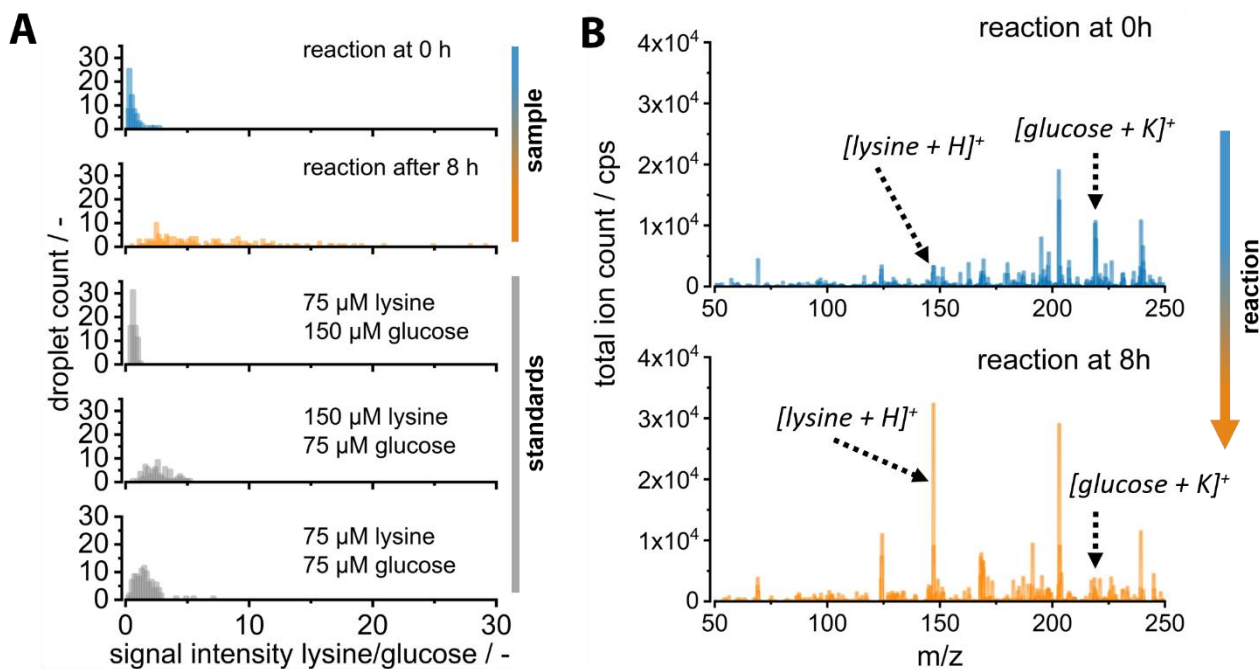


Figure 5. (A) Conversion ratio of corresponding signals of product (lysine) and substrate (glucose) of single droplets for a sample at the reaction start and after eight hours, and for artificial standards with lysine/glucose ratios of 1:2, 2:1 and 1:1 ($N_{0h}=70$, $N_{8h}=136$, $N_{1:2}=75$, $N_{2:1}=73$, $N_{1:1}=102$). (B) Mass spectrum of a corresponding droplet at start and after eight hours with marked m/z values for the corresponding lysine and glucose ion signals.

means that biocatalysis will become quantifiable at the level of the minimal catalytic unit, the single cell. The developed analytical concept was also proven extendable to other types of cell catalysts by customizing the buffer medium to cell-specific needs such as pH, ionic strength and volatility. With the proposed droplet-chip/MS platform, different hurdles lay on the way to single-cell resolution. This challenge can be tackled by using more powerful state-of-the-art MS instruments with highest sensitivities, e. g. triple quadrupole MS instruments for targeted analyses, while time-of-flight analyzers will be useful for non-targeted analyses. Moreover, a reduction of ion suppression by further decreasing the buffer salt concentrations might enhance the sensitivity of the method. Adapting the platform to advanced emitter technologies (i. e. full-body glass chips with monolithical emitters), or by employing novel desalting strategies might further enhance signal-to-noise ratios. Implementing on-chip temperature control for increasing cell-specific L-lysine production rates and

before. It is likely that *hitherto* unknown cell-to-cell heterogeneities in terms of rates and yields will become quantifiable. But what is needed to reach the single-cell level and to quantitatively probe biocatalysis of the minimal living catalytic unit? We speculate that with the combination of improved on-chip incubation strategies, further medium optimization and enhanced chip/MS interface technology, e.g. mass-activated droplet sorting⁶² for subsequent cell cultivation the reactivity of a single biocatalyst will become analytically accessible. It is only at this scale, that complex mechanisms controlling the efficiency of whole-cell biocatalysts can be understood. Further improvements will include the massive parallelization of droplet incubation in order to analyze single cells with even higher throughput. As the developed method is label-free, the analytical target window can now be expanded to a wealth of catalytically relevant molecules and cell types, with potential applications in biotechnology, life and medical sciences, and organic chemistry.

■ ASSOCIATED CONTENT

Supporting Information

MS response of lysine in complex and volatile reaction media; activity assays of used strains of *E. coli*, *H. polymorpha* and *C. glutamicum*; cell encapsulation efficiency; droplet shrinkage during incubation; MS response of lysine standards; chemicals.

■ AUTHOR INFORMATION

Corresponding Author

Christian Dusny - Helmholtz-Centre for Environmental Research - UFZ Leipzig - Leipzig, Germany

* Email: christian.dusny@ufz.de

Authors

Martin Schirmer - Helmholtz-Centre for Environmental Research - UFZ Leipzig - Leipzig, Germany

Konstantin Wink - Institute of Analytical Chemistry - Leipzig University - Leipzig, Germany

Stefan Ohla - Institute of Analytical Chemistry - Leipzig University - Leipzig, Germany

Detlev Belder - Institute of Analytical Chemistry - Leipzig University - Leipzig, Germany

Andreas Schmid - Helmholtz-Centre for Environmental Research - UFZ Leipzig - Leipzig, Germany

Author Contributions

#MS and KW contributed equally to this work.

Notes

The authors declare no competing financial interest.

■ ACKNOWLEDGEMENTS

This work was funded by the Deutsche Forschungsgemeinschaft (DFG, German Research Foundation)—FOR 2177—project number 251124697. We thank Sebastian Piendl for his help with the electromagnetic shielding of the chip. We are also grateful to Ron Stauder for his assistance with the HPLC analytics.

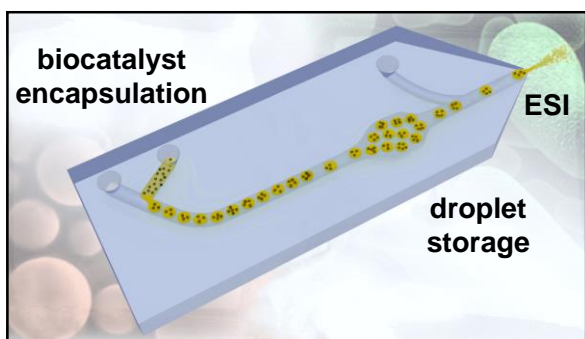
■ REFERENCES

- (1) de Carvalho, C. C. C. R. Whole Cell Biocatalysts: Essential Workers from Nature to the Industry. *Microbial Biotechnology* **2017**, *10* (2), 250–263. <https://doi.org/10.1111/1751-7915.12363>.
- (2) Lin, B.; Tao, Y. Whole-Cell Biocatalysts by Design. *Microbial Cell Factories* **2017**, *16* (1), 106. <https://doi.org/10.1186/s12934-017-0724-7>.
- (3) Gröger, H.; Hummel, W. Combining the ‘Two Worlds’ of Chemocatalysis and Biocatalysis towards Multi-Step One-Pot Processes in Aqueous Media. *Current Opinion in Chemical Biology* **2014**, *19*, 171–179. <https://doi.org/10.1016/J.CBPA.2014.03.002>.
- (4) Krone, K. M.; Warias, R.; Ritter, C.; Li, A.; Acevedo-Rocha, C. G.; Reetz, M. T.; Belder, D. Analysis of Enantioselective Biotransformations Using a Few Hundred Cells on an Integrated Microfluidic Chip. *Journal of the American Chemical Society* **2016**, *138* (7), 2102–2105. <https://doi.org/10.1021/jacs.5b12443>.
- (5) Schrewe, M.; Julsing, M. K.; Bühler, B.; Schmid, A. Whole-Cell Biocatalysis for Selective and Productive C–O Functional Group Introduction and Modification. *Chemical Society Reviews* **2013**, *42* (15), 6346. <https://doi.org/10.1039/c3cs6001d>.
- (6) Ratnayake, N. D.; Theisen, C.; Walter, T.; Walker, K. D. Whole-Cell Biocatalytic Production of Various Substituted β -Aryl- and β -Heteroaryl- β -Amino Acids. *Journal of Biotechnology* **2016**, *217*, 12–21. <https://doi.org/10.1016/J.JBIOTECH.2015.10.012>.
- (7) Müller, C. A.; Dennig, A.; Welters, T.; Winkler, T.; Ruff, A. J.; Hummel, W.; Gröger, H.; Schwaneberg, U. Whole-Cell Double Oxidation of n-Heptane. *Journal of Biotechnology* **2014**, *191*, 196–204. <https://doi.org/10.1016/J.JBIOTECH.2014.06.001>.
- (8) Weber, N.; Gorwa-Grauslund, M.; Carlquist, M. Engineered Baker’s Yeast as Whole-Cell Biocatalyst for One-Pot Stereo-Selective Conversion of Amines to Alcohols. *Microbial Cell Factories* **2014**, *13* (1), 118. <https://doi.org/10.1186/s12934-014-0118-z>.
- (9) Ibáñez, A. J.; Fagerer, S. R.; Schmidt, A. M.; Urban, P. L.; Jefimovs, K.; Geiger, P.; Dechant, R.; Heinemann, M.; Zenobi, R. Mass Spectrometry-Based Metabolomics of Single Yeast Cells. *Proceedings of the National Academy of Sciences of the United States of America* **2013**, *110* (22), 8790–8794. <https://doi.org/10.1073/pnas.1209302110>.
- (10) Zenobi, R. Single-Cell Metabolomics: Analytical and Biological Perspectives. *Science (New York, N.Y.)* **2013**, *342* (6163), 1243259. <https://doi.org/10.1126/science.1243259>.
- (11) Dittrich, P.; Jakubowski, N. Current Trends in Single Cell Analysis. *Analytical and Bioanalytical Chemistry* **2014**, *406* (27), 6957–6961. <https://doi.org/10.1007/s00216-014-8163-3>.
- (12) Comi, T. J.; Do, T. D.; Rubakhin, S. S.; Sweedler, J. V. Categorizing Cells on the Basis of Their Chemical Profiles: Progress in Single-Cell Mass Spectrometry. *Journal of the American Chemical Society* **2017**, *139* (11), 3920–3929. <https://doi.org/10.1021/jacs.6b12822>.
- (13) Dusny, C.; Lohse, M.; Reemtsma, T.; Schmid, A.; Lechtenfeld, O. J. Quantifying a Biocatalytic Product from a Few Living Microbial Cells Using

- Microfluidic Cultivation Coupled to FT-ICR-MS. *Analytical Chemistry* **2019**, *91* (11), 7012–7018. <https://doi.org/10.1021/acs.analchem.9b00978>.
- (14) Kempa, E. E.; Hollywood, K. A.; Smith, C. A.; Barran, P. E. High Throughput Screening of Complex Biological Samples with Mass Spectrometry – from Bulk Measurements to Single Cell Analysis. *The Analyst* **2019**, *144* (3), 872–891. <https://doi.org/10.1039/C8AN01448E>.
- (15) Binder, D.; Drepper, T.; Jaeger, K.-E.; Delvigne, F.; Wiechert, W.; Kohlheyer, D.; Grünberger, A. Homogenizing Bacterial Cell Factories: Analysis and Engineering of Phenotypic Heterogeneity. *Metabolic Engineering* **2017**, *42*, 145–156. <https://doi.org/10.1016/j.ymben.2017.06.009>.
- (16) Gruenberger, A.; Probst, C.; Heyer, A.; Wiechert, W.; Frunzke, J.; Kohlheyer, D. Microfluidic Picoliter Bioreactor for Microbial Single-Cell Analysis: Fabrication, System Setup, and Operation Video Link. *J. Vis. Exp* **2013**, *8250560* (10). <https://doi.org/10.3791/50560>.
- (17) Hümmer, D.; Kurth, F.; Naredi-Rainer, N.; Dittrich, P. S. Single Cells in Confined Volumes: Microchambers and Microdroplets. *Lab on a Chip*. The Royal Society of Chemistry January 26, 2016, pp 447–458. <https://doi.org/10.1039/c5lc01314c>.
- (18) Shembekar, N.; Chaipan, C.; Utharala, R.; Merten, C. A. Droplet-Based Microfluidics in Drug Discovery, Transcriptomics and High-Throughput Molecular Genetics. *Lab on a Chip* **2016**, *16* (8), 1314–1331. <https://doi.org/10.1039/C6LC00249H>.
- (19) Nichols, D.; Cahoon, N.; Trakhtenberg, E. M.; Pham, L.; Mehta, A.; Belanger, A.; Kanigan, T.; Lewis, K.; Epstein, S. S. Use of Ichip for High-Throughput in Situ Cultivation of “Uncultivable” Microbial Species. *Applied and environmental microbiology* **2010**, *76* (8), 2445–2450. <https://doi.org/10.1128/AEM.01754-09>.
- (20) Mahler, L.; Wink, K.; Beulig, R. J.; Scherlach, K.; Tovar, M.; Zang, E.; Martin, K.; Hertweck, C.; Belder, D.; Roth, M. Detection of Antibiotics Synthetized in Microfluidic Picolitre-Droplets by Various Actinobacteria. *Scientific Reports* **2018**, *8* (1), 13087. <https://doi.org/10.1038/s41598-018-31263-2>.
- (21) Fritsch, F. S. O.; Rosenthal, K.; Kampert, A.; Howitz, S.; Dusny, C.; Blank, L. M.; Schmid, A. Picoliter NDEP Traps Enable Time-Resolved Contactless Single Bacterial Cell Analysis in Controlled Microenvironments. *Lab Chip* **2013**, *13* (3), 397–408. <https://doi.org/10.1039/C2LC41092C>.
- (22) Kempa, E. E.; Hollywood, K. A.; Smith, C. A.; Barran, P. E. High Throughput Screening of Complex Biological Samples with Mass Spectrometry – from Bulk Measurements to Single Cell Analysis. *Analyst* **2019**, *144* (3), 872–891. <https://doi.org/10.1039/C8AN01448E>.
- (23) Shang, L.; Cheng, Y.; Zhao, Y. Emerging Droplet Microfluidics. *Chemical Reviews* **2017**, *117* (12), 7964–8040. <https://doi.org/10.1021/acs.chemrev.6b00848>.
- (24) Theberge, A. B.; Courtois, F.; Schaerli, Y.; Fischlechner, M.; Abell, C.; Hollfelder, F.; Huck, W. T. S. Microdroplets in Microfluidics: An Evolving Platform for Discoveries in Chemistry and Biology. *Angewandte Chemie International Edition* **2010**, *49* (34), 5846–5868. <https://doi.org/10.1002/anie.200906653>.
- (25) Kaminski, T. S.; Garstecki, P. Controlled Droplet Microfluidic Systems for Multistep Chemical and Biological Assays. *Chemical Society Reviews* **2017**, *46* (20), 6210–6226. <https://doi.org/10.1039/C5CS00717H>.
- (26) Baret, J.-C.; Miller, O. J.; Taly, V.; Ryckelynck, M.; El-Harrak, A.; Frenz, L.; Rick, C.; Samuels, M. L.; Hutchison, J. B.; Agresti, J. J.; Link, D. R.; Weitz, D. A.; Griffiths, A. D. Fluorescence-Activated Droplet Sorting (FADS): Efficient Microfluidic Cell Sorting Based on Enzymatic Activity. *Lab on a Chip* **2009**, *9* (13), 1850. <https://doi.org/10.1039/b902504a>.
- (27) Cole, R. H.; de Lange, N.; Gartner, Z. J.; Abate, A. R. Compact and Modular Multicolour Fluorescence Detector for Droplet Microfluidics. *Lab on a Chip* **2015**, *15* (13), 2754–2758. <https://doi.org/10.1039/C5LC00333D>.
- (28) Theberge, A. B.; Whyte, G.; Frenzel, M.; Fidalgo, L. M.; Wootton, R. C. R.; Huck, W. T. S. Suzuki-Miyaura Coupling Reactions in Aqueous Microdroplets with Catalytically Active Fluorous Interfaces. *Chemical Communications* **2009**, No. 41, 6225. <https://doi.org/10.1039/b911594c>.
- (29) Price, A. K.; Paegel, B. M. Discovery in Droplets. *Analytical Chemistry* **2016**, *88* (1), 339–353. <https://doi.org/10.1021/acs.analchem.5b04139>.
- (30) Fidalgo, L. M.; Whyte, G.; Ruotolo, B. T.; Benesch, J. L. P.; Stengel, F.; Abell, C.; Robinson, C. V.; Huck, W. T. S. Coupling Microdroplet Microreactors with Mass Spectrometry: Reading the Contents of Single Droplets Online. *Angewandte Chemie International Edition* **2009**, *48* (20), 3665–3668. <https://doi.org/10.1002/anie.200806103>.
- (31) Sun, S.; Kennedy, R. T. Droplet Electrospray Ionization Mass Spectrometry for High Throughput Screening for Enzyme Inhibitors. *Analytical Chemistry* **2014**, *86* (18), 9309–9314. <https://doi.org/10.1021/ac502542z>.
- (32) Gasilova, N.; Yu, Q.; Qiao, L.; Girault, H. H. On-Chip Spyhole Mass Spectrometry for Droplet-Based Microfluidics. *Angewandte Chemie International Edition* **2014**, *53* (17), 4408–4412. <https://doi.org/10.1002/anie.201310795>.
- (33) Küster, S. K.; Fagerer, S. R.; Verboket, P. E.; Eyer, K.; Jefimovs, K.; Zenobi, R.; Dittrich, P. S. Interfacing Droplet Microfluidics with Matrix-Assisted Laser Desorption/Ionization Mass Spectrometry: Label-Free Content Analysis of

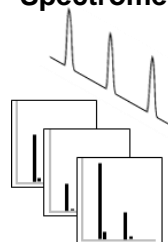
- (34) Single Droplets. *Analytical Chemistry* **2013**, *85* (3), 1285–1289. <https://doi.org/10.1021/ac3033189>.
Smith, C. A.; Li, X.; Mize, T. H.; Sharpe, T. D.; Graziani, E. I.; Abell, C.; Huck, W. T. S. Sensitive, High Throughput Detection of Proteins in Individual, Surfactant-Stabilized Picoliter Droplets Using Nanoelectrospray Ionization Mass Spectrometry. *Analytical Chemistry* **2013**, *85* (8), 3812–3816. <https://doi.org/10.1021/ac400453t>.
- (35) Kelly, R. T.; Page, J. S.; Marginean, I.; Tang, K.; Smith, R. D. Dilution-Free Analysis from Picoliter Droplets by Nano-Electrospray Ionization Mass Spectrometry. *Angewandte Chemie International Edition* **2009**, *48* (37), 6832–6835. <https://doi.org/10.1002/anie.200902501>.
- (36) Keilhauer, C.; Eggeling, L.; Sahm, H. Isoleucine Synthesis in *Corynebacterium Glutamicum*: Molecular Analysis of the IlvB-IlvN-IlvC Operon. *Journal of Bacteriology* **1993**, *175* (17), 5595–5603. <https://doi.org/10.1128/jb.175.17.5595-5603.1993>.
- (37) Jakiela, S.; Kaminski, T. S.; Cybulski, O.; Weibel, D. B.; Garstecki, P. Bacterial Growth and Adaptation in Microdroplet Chemostats. *Angewandte Chemie International Edition* **2013**, *52* (34), 8908–8911. <https://doi.org/10.1002/anie.201301524>.
- (38) Liu, X.; Painter, R. E.; Enesa, K.; Holmes, D.; Whyte, G.; Garlisi, C. G.; Monsma, F. J.; Rehak, M.; Craig, F. F.; Smith, C. A. High-Throughput Screening of Antibiotic-Resistant Bacteria in Picodroplets. *Lab on a Chip* **2016**, *16* (9), 1636–1643. <https://doi.org/10.1039/C6LC00180G>.
- (39) Iavarone, A. T.; Udekwu, O. A.; Williams, E. R. Buffer Loading for Counteracting Metal Salt-Induced Signal Suppression in Electrospray Ionization. *Anal. Chem.* **2004**, *76* (14), 3944–3950. <https://doi.org/10.1021/ac049724+>.
- (40) Becker, J.; Zelder, O.; Häfner, S.; Schröder, H.; Wittmann, C. From Zero to Hero—Design-Based Systems Metabolic Engineering of *Corynebacterium Glutamicum* for L-Lysine Production. *Metabolic Engineering* **2011**, *13* (2), 159–168. <https://doi.org/10.1016/j.YMBEN.2011.01.003>.
- (41) Rosenthal, K.; Falke, F.; Frick, O.; Dusny, C.; Schmid, A.; Rosenthal, K.; Falke, F.; Frick, O.; Dusny, C.; Schmid, A. An Inert Continuous Microreactor for the Isolation and Analysis of a Single Microbial Cell. *Micromachines* **2015**, *6* (12), 1836–1855. <https://doi.org/10.3390/mi6121459>.
- (42) Gruenberger, A.; Ooyen, J. van; Paczia, N.; Rohe, P.; Schiendzielorz, G.; Eggeling, L.; Wiechert, W.; Kohlheyer, D.; Noack, S. Beyond Growth Rate 0.6: *Corynebacterium Glutamicum* Cultivated in Highly Diluted Environments. *Biotechnology and Bioengineering* **2013**, *110* (1), 220–228. <https://doi.org/10.1002/bit.24616>.
- (43) Beulig, R. J.; Warias, R.; Heiland, J. J.; Ohla, S.; Zeitler, K.; Belder, D. A Droplet-Chip/Mass Spectrometry Approach to Study Organic Synthesis at Nanoliter Scale. *Lab on a Chip* **2017**, *17* (11), 1996–2002. <https://doi.org/10.1039/C7LC00313G>.
- (44) Dusny, C.; Schmid, A. The MOX Promoter in *Hansenula Polymorpha* Is Ultrasensitive to Glucose-Mediated Carbon Catabolite Repression. *FEMS Yeast Research* **2016**, *16* (6). <https://doi.org/10.1093/femsyr/fow067>.
- (45) Theodosiou, E.; Frick, O.; Bühler, B.; Schmid, A. Metabolic Network Capacity of *Escherichia Coli* for Krebs Cycle-Dependent Proline Hydroxylation. *Microbial Cell Factories* **2015**, *14* (1), 108. <https://doi.org/10.1186/s12934-015-0298-1>.
- (46) Collins, D. J.; Neild, A.; deMello, A.; Liu, A.-Q.; Ai, Y. The Poisson Distribution and beyond: Methods for Microfluidic Droplet Production and Single Cell Encapsulation. *Lab on a Chip* **2015**, *15* (17), 3439–3459. <https://doi.org/10.1039/C5LC00614G>.
- (47) Wink, K.; Mahler, L.; Beulig, J. R.; Piendl, S. K.; Roth, M.; Belder, D. An Integrated Chip-Mass Spectrometry and Epifluorescence Approach for Online Monitoring of Bioactive Metabolites from Incubated Actinobacteria in Picoliter Droplets. *Anal Bioanal Chem* **2018**, *410* (29), 7679–7687. <https://doi.org/10.1007/s00216-018-1383-1>.
- (48) Xiao, Y.; Bowen, C. H.; Liu, D.; Zhang, F. Exploiting Nongenetic Cell-to-Cell Variation for Enhanced Biosynthesis. *Nature Chemical Biology* **2016**, *12* (5), 339–344. <https://doi.org/10.1038/nchembio.2046>.
- (49) Wang, B. L.; Ghaderi, A.; Zhou, H.; Agresti, J.; Weitz, D. A.; Fink, G. R.; Stephanopoulos, G. Microfluidic High-Throughput Culturing of Single Cells for Selection Based on Extracellular Metabolite Production or Consumption. *Nature Biotechnology* **2014**, *32* (5), 473–478. <https://doi.org/10.1038/nbt.2857>.
- (50) Meyer, A.; Pellaux, R.; Potot, S.; Becker, K.; Hohmann, H.-P.; Panke, S.; Held, M. Optimization of a Whole-Cell Biocatalyst by Employing Genetically Encoded Product Sensors inside Nanolitre Reactors. *Nature Chemistry* **2015**, *7* (8), 673–678. <https://doi.org/10.1038/nchem.2301>.
- (51) van Tatenhove-Pel, R. J.; Hernandez-Valdes, J. A.; Teusink, B.; Kuipers, O. P.; Fischlechner, M.; Bachmann, H. Microdroplet Screening and Selection for Improved Microbial Production of Extracellular Compounds. *Current Opinion in Biotechnology* **2020**, *61*, 72–81. <https://doi.org/10.1016/j.copbio.2019.10.007>.
- (52) Follmann, M.; Ochrombel, I.; Krämer, R.; Trötschel, C.; Poetsch, A.; Rückert, C.; Hüser, A.; Persicke, M.; Seiferling, D.; Kalinowski, J.; Marin, K. Functional Genomics of PH Homeostasis in *Corynebacterium Glutamicum* Revealed Novel Links between PH Response, Oxidative Stress,

- Iron Homeostasis and Methionine Synthesis. *BMC Genomics* **2009**, *10* (1), 621. <https://doi.org/10.1186/1471-2164-10-621>.
- (53) Razak, M. A.; Viswanath, B. Comparative Studies for the Biotechnological Production of L-Lysine by Immobilized Cells of Wild-Type *Corynebacterium Glutamicum* ATCC 13032 and Mutant MH 20-22 B. *3 Biotech* **2015**, *5* (5), 765–774. <https://doi.org/10.1007/s13205-015-0275-8>.
- (54) Fränzel, B.; Trötschel, C.; Rückert, C.; Kalinowski, J.; Poetsch, A.; Wolters, D. A. Adaptation of *Corynebacterium Glutamicum* to Salt-Stress Conditions. *PROTEOMICS* **2010**, *10* (3), 445–457. <https://doi.org/10.1002/pmic.200900482>.
- (55) Blombach, B.; Buchholz, J.; Busche, T.; Kalinowski, J.; Takors, R. Impact of Different CO₂/HCO₃⁻ Levels on Metabolism and Regulation in *Corynebacterium Glutamicum*. *Journal of Biotechnology* **2013**, *168* (4), 331–340. <https://doi.org/10.1016/j.jbiotec.2013.10.005>.
- (56) Hollenberg, C. P.; Gellissen, G. Production of Recombinant Proteins by Methylophilic Yeasts. *Current Opinion in Biotechnology* **1997**, *8* (5), 554–560. [https://doi.org/10.1016/S0958-1669\(97\)80028-6](https://doi.org/10.1016/S0958-1669(97)80028-6).
- (57) Varela, C. A.; Baez, M. E.; Agosin, E. Osmotic Stress Response: Quantification of Cell Maintenance and Metabolic Fluxes in a Lysine-Overproducing Strain of *Corynebacterium Glutamicum*. *Appl. Environ. Microbiol.* **2004**, *70* (7), 4222–4229. <https://doi.org/10.1128/AEM.70.7.4222-4229.2004>.
- (58) Hamza, M. A.; Serratrice, G.; Stebe, M. J.; Delpuech, J. J. Solute-Solvent Interactions in Perfluorocarbon Solutions of Oxygen. An NMR Study. *Journal of the American Chemical Society* **1981**, *103* (13), 3733–3738. <https://doi.org/10.1021/ja00403a020>.
- (59) Steyer, D. J.; Kennedy, R. T. High-Throughput Nanoelectrospray Ionization-Mass Spectrometry Analysis of Microfluidic Droplet Samples. *Anal. Chem.* **2019**, *91* (10), 6645–6651. <https://doi.org/10.1021/acs.analchem.9b00571>.
- (60) Wei, Z.; Wleklinski, M.; Ferreira, C.; Cooks, R. G. Reaction Acceleration in Thin Films with Continuous Product Deposition for Organic Synthesis. *Angewandte Chemie International Edition* **2017**, *56* (32), 9386–9390. <https://doi.org/10.1002/anie.201704520>.
- (61) Chen, S.; Wan, Q.; Badu-Tawiah, A. K. Picomole-Scale Real-Time Photoreaction Screening: Discovery of the Visible-Light-Promoted Dehydrogenation of Tetrahydroquinolines under Ambient Conditions. *Angewandte Chemie International Edition* **2016**, *55* (32), 9345–9349. <https://doi.org/10.1002/anie.201603530>.
- (62) Holland-Moritz, D. A.; Wismer, M.; Mann, B.; Farasat, I.; Guetschow, E.; Sun, S.; Moore, J.; Kennedy, R.; Mangion, I.; Welch, C. J.; Devine, P. Mass Activated Droplet Sorting (MADS) Enables High Throughput Screening of Enzymatic Reactions at Nanoliter Scale. *Angewandte Chemie International Edition* *n/a* (n/a). <https://doi.org/10.1002/anie.201913203>.
-



microfluidic droplet-chip

Mass Spectrometry



Whole-cell heterogeneity

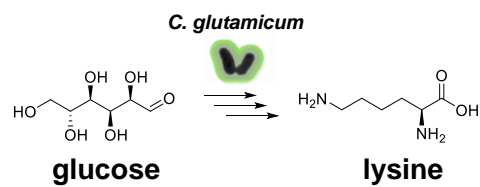
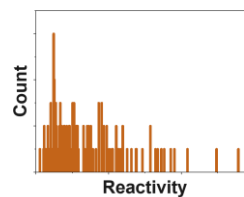


Table of content (TOC)